

Activation of the West Nile virus NS3 protease: Molecular dynamics evidence for a conformational selection mechanism

Dariusz Ekonomiuk and Amedeo Caffisch*

Department of Biochemistry, University of Zurich, CH-8057 Zurich, Switzerland

Received 19 December 2008; Revised 16 February 2009; Accepted 17 February 2009

DOI: 10.1002/pro.1110

Published online 16 March 2009 proteinscience.org

Abstract: The flaviviral nonstructural 3 protease (NS3pro) is essential for virus replication and is therefore a pharmaceutically relevant target to fight Dengue and West Nile virus (WNV). NS3pro is a chymotrypsin-like serine protease which requires a polypeptide cofactor (NS2B) for activation. Recent X-ray crystallography studies have led to the suggestion that the substrate binds to the two-component NS2B-NS3pro enzyme by an induced-fit mechanism. Here, multiple explicit water molecular dynamics simulations of the WNV NS2B-NS3pro enzyme show that the active conformation of the NS2B cofactor (in which its β -loop is part of the substrate binding site) is stable over a 50-ns time scale even in the absence of the inhibitor. The partial and reversible opening of the NS2B β -loop and its correlated motion with an adjacent NS3pro loop, both observed in the simulations started from the active conformation, are likely to facilitate substrate binding and product release. Moreover, in five of eight simulations without inhibitor (started from two X-ray structures both with improperly formed oxyanion hole) the Thr132-Gly133 peptide bond flips spontaneously thereby promoting the formation of the catalytically competent oxyanion hole, which then stays stable until the end of the runs. The simulation results provide evidence at atomic level of detail that the substrate binds to the NS2B-NS3pro enzyme by conformational selection, rather than induced-fit mechanism.

Keywords: protein simulations; conformational selection; flaviviral protease; West Nile virus; Dengue virus; oxyanion hole

INTRODUCTION

There are currently neither vaccines nor safe drugs to fight the pathogenic members of the flavivirus family like West Nile virus (WNV) and the closely related Dengue virus, which are transmitted by mosquito bites. Despite an estimated 2.5 billion people are potential victims of encephalitis and other fatal mal-

adies caused by flaviviruses,¹ these diseases have received much less attention than other tropical diseases like avian influenza probably because mosquitoes can fly only much shorter distances than migratory birds, and flaviviruses are widespread mainly in poor countries. Recently, the nonstructural 3 protease (NS3pro) has been shown to be responsible for cleavage of the viral polyprotein precursor and to play a pivotal role in the replication of flaviviruses.^{2,3} In fact, site directed mutagenesis focused on the NS3pro cleavage sites in the polyprotein precursor abolishes viral infectivity.³ Therefore, NS3pro is one of the most promising targets for drug development against flaviviridae infections. In this context, it is important to note that two inhibitors of the closely related hepatitis C virus protease are under late-stage clinical development.⁴⁻⁷

Additional Supporting Information may be found in the online version of this article.

Abbreviations: BPTI, bovine pancreatic trypsin inhibitor; MD, molecular dynamics; NS3pro, nonstructural 3 protease; RMSD, root mean square deviation; WNV, West Nile virus.

Grant sponsor: Swiss National Science Foundation.

*Correspondence to: Amedeo Caffisch, Department of Biochemistry, University of Zurich, Winterthurerstrasse 190, CH-8057 Zurich, Switzerland. E-mail: caffisch@bioc.uzh.ch

Table I. Summary of the MD Simulations

Starting structure ^a	PDB code	With inhibitor	Number of simulations ^b	Length (ns)	C _α RMSD ^c (Å)
Active	2fp7	Yes	3	35, 30, 15	1.3, 1.4, 1.2
Active	2fp7	No	4	80, 30, 20, 15	1.2, 1.8, 1.2, 1.3
Inactive	2ggv	No	4	80, 80, 40, 30	1.7, 1.7, 1.3, 1.2

^a The designations active and inactive are used to specify the conformations of the NS2B cofactor with its $\beta 2$ - $\beta 3$ loop close to the active site and far away from it, respectively.

^b Duplicate runs were started using different seeds for the random distribution of the initial velocities.

^c Value of the C_α RMSD averaged over the last 10 ns. The C_α atoms of NS3pro were used to calculate the RMSD except for the segment 28–32, which is missing in the 2fp7 structure, and the loops B2B-C2 and E2B-F2 which are flexible.

The flaviviral NS3pro chain adopts a chymotrypsin-like fold with two six-stranded β -barrels. The binding pocket is small and very shallow with the catalytic triad (His51-Asp75-Ser135) located at the cleft between the two β -barrels.⁸ It has been reported that the catalytic activity of NS3pro is significantly increased by the presence of a 47-residue region of the nonstructural cofactor 2B (NS2B).⁹ Two X-ray structures of WNV NS2B-NS3pro in complex with inhibitors have been solved: One with the substrate-based tetrapeptide benzoyl-norleucine-lysine-arginine-arginine-aldehyde (Bz-Nle-Lys-Arg-Arg-H, PDB code 2fp7)⁸ and the other with bovine pancreatic trypsin inhibitor (BPTI, PDB code 2ijo).¹⁰ Despite the very different size of the two inhibitors, these two X-ray structures show essentially identical conformations of the NS2B-NS3pro complex except for the oxyanion hole which is in the catalytically competent state only in the complex with BPTI.

The coordinates of inhibitor-bound and -free NS3pro (but not NS2B) are closely superposable with a root mean square deviation (RMSD) of only 0.8 Å for 148 of 151 C_α atoms.¹⁰ On the other hand, there is a remarkable difference in the location of the $\beta 2$ - $\beta 3$ loop of NS2B. This loop is part of the substrate binding site in both inhibitor-bound structures whereas in the inhibitor-free structure (PDB code 2ggv) its tip is located at a distance of about 50 Å from the active site and protrudes towards the solvent. On the basis of this difference as well as the nonproductive conformation of the oxyanion hole in the complex with the tetrapeptide inhibitor, it has been suggested that activation obeys an induced-fit mechanism.¹⁰

Here, explicit water molecular dynamics (MD) simulations are performed to investigate the flexibility and relative stability of the putative initial and final structures of this mechanism. Multiple MD runs are started from the inhibitor-free and inhibitor-bound conformations for a total simulation time of 0.46 μ s. The stability of the catalytically competent oxyanion hole structure and of the conformation with the NS2B $\beta 2$ - $\beta 3$ loop making part of the substrate binding site provides evidence that (poly)peptide substrate and inhibitors bind by conformational selection rather

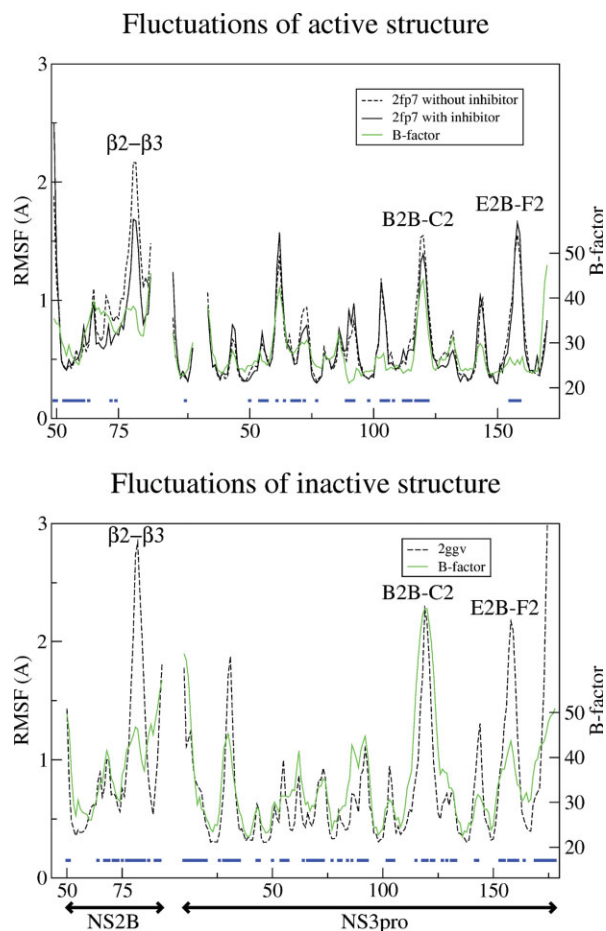


Figure 1. Root mean square fluctuations (RMSF) of C_α atoms in Å (black lines with y-axis on the left) and crystallographic B-factors (green line with y-axis on the right) as a function of residue number. The RMSF values are average values over simulation intervals of 5 ns (excluding the first 5 ns). Crystal contacts are shown by blue squares for residues with one or more heavy atoms closer than 5 Å to heavy atoms of neighboring proteins in the crystal. The secondary structure assignment and residue numbering of Aleshin *et al.* are used,¹⁰ that is, the $\beta 2$ - $\beta 3$ loop of NS2B consists of residues Leu79-Phe85, while the loops E1B-F1, B2B-C2, and E2B-F2 of NS3pro consist of residues Tyr68-Cys78, Lys117-Glu122, and Val154-Ile162, respectively. [Color figure can be viewed in the online issue, which is available at www.interscience.wiley.com.]

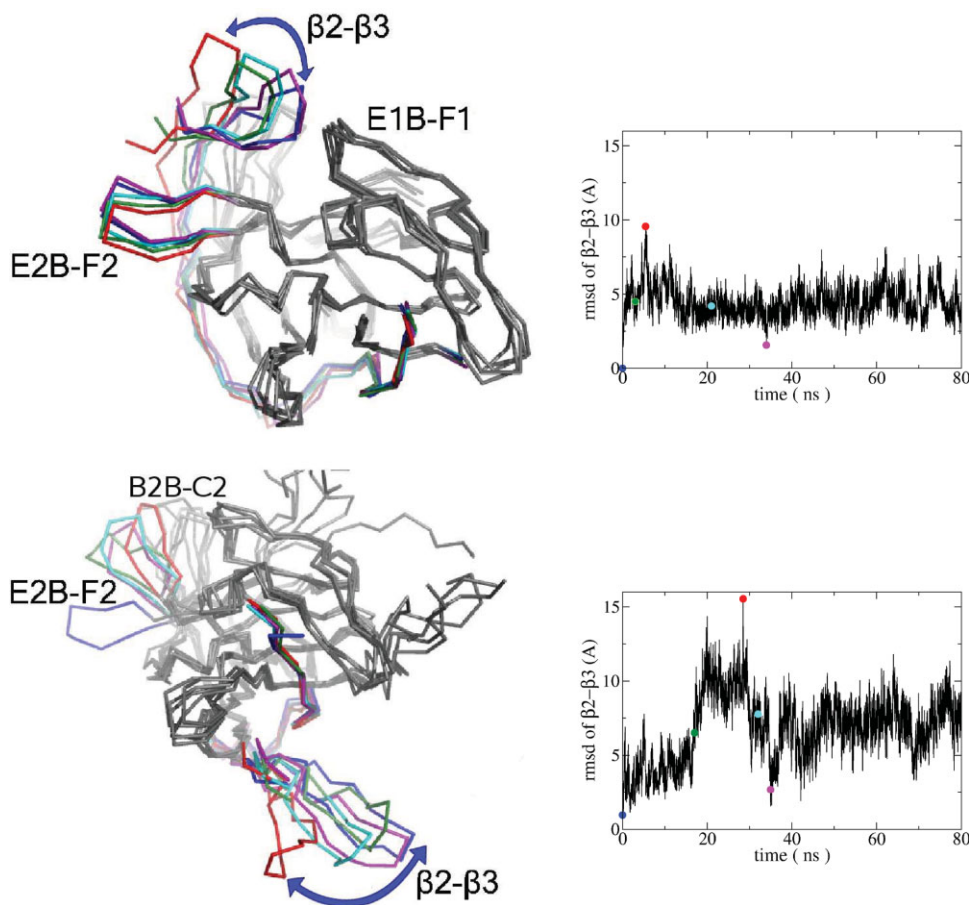


Figure 2. Flexibility of the $\beta 2$ - $\beta 3$ loop of NS2B in the absence of the inhibitor. Selected snapshots (left) and time series of RMSD of C_{α} atoms 79–85 of NS2B (right) are shown for the 80-ns runs started from the active (top) and inactive (bottom) conformation. Different colors are used for the NS2B chain and the E2B-F2 loop of NS3pro in both individual snapshots and the corresponding data points along the time series. Time series of all other MD runs are in the Supporting Information Fig. S2. [Color figure can be viewed in the online issue, which is available at www.interscience.wiley.com.]

than induced-fit. Moreover, the partial opening of the NS2B $\beta 2$ - $\beta 3$ loop and its correlated motion with an adjacent loop of NS3pro are likely to promote substrate binding and product release as these two loops make up the nonprime part of the substrate binding site.

Results

Table I lists the simulations performed as well as their length and RMSD. The conformation of the NS2B cofactor in the X-ray structure with the tetrapeptide-aldehyde inhibitor (*2fp7*) is called active hereafter because the NS2B $\beta 2$ - $\beta 3$ loop is part of the active site and because of the previously reported deleterious effects of mutations in this loop on the catalytic activity.¹¹ In the following, the analysis focuses on the runs without the inhibitor unless explicitly mentioned. The secondary structure assignment and residue numbering of Aleshin *et al.* are used,¹⁰ that is, the $\beta 2$ - $\beta 3$ loop of NS2B consists of residues Leu79-Phe85, while the loops E1B-F1, B2B-C2, and E2B-F2 of NS3pro consist of residues Tyr68-Cys78, Lys117-Glu122, and Val154-Ile162, respectively.

Overall stability and flexibility

The low values of the C_{α} RMSD from the X-ray structure used as starting conformation indicate that the overall stability is preserved in all MD runs (Table I and Supporting Information Fig. S1). Furthermore, there is a very high correlation between the C_{α} atomic fluctuations calculated along the MD simulations and the crystallographic temperature factors (see Fig. 1), except for the E2B-F2 loop in NS3pro and the $\beta 2$ - $\beta 3$ loop in NS2B. Note that these discrepancies can be explained by the contacts with atoms in neighboring proteins which restrict the motion of the aforementioned loops in the crystal (PDB codes *2fp7* and *2ggv*) but are not present in the MD simulations. The low RMSD values and reasonable fluctuations indicate that the force field and simulation protocol are adequate for investigating the structural plasticity of the WNV NS2B-NS3pro complex. In recent MD simulations with a different force field,¹² RMSD values of about 2.5 Å were observed in a 10-ns run started from the inactive conformation of the NS2B-NS3pro complex of the Dengue virus (PDB code *2fom*). On the other hand, Zuo *et al.* did not carry out MD simulations

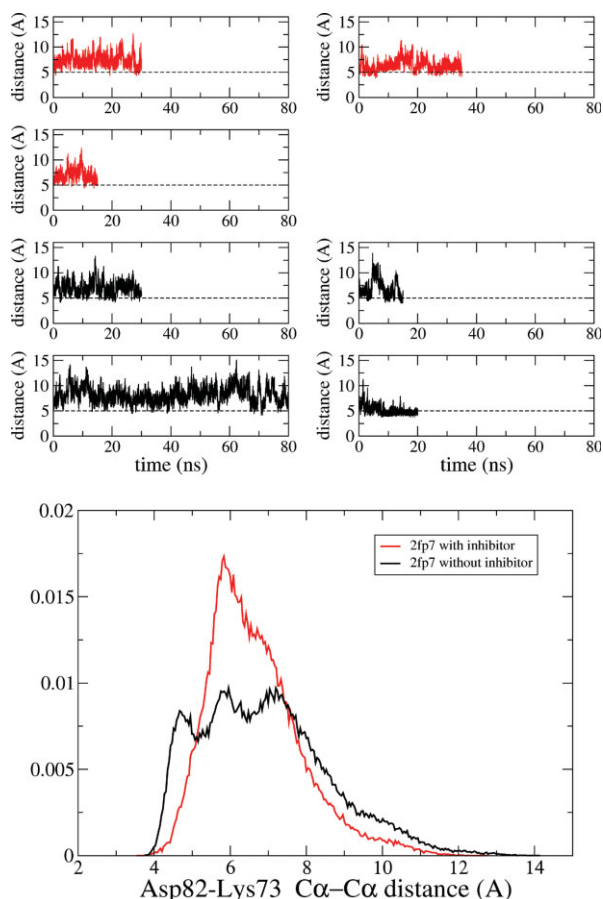


Figure 3. Time series (top) and distribution (bottom) of the NS2B Asp82-NS3pro Lys73 C_{α} - C_{α} distance, which is the distance between the tips of the β 2- β 3 loop of NS2B and the E1B-F1 loop of NS3pro. [Color figure can be viewed in the online issue, which is available at www.interscience.wiley.com.]

starting from the active conformation of the complex. Yet, the main conclusion of their study that the NS2B cofactor is essential for substrate binding¹² is consistent with our results (see below).

Stability of the NS2B cofactor structure in its active conformation

The active conformation of the NS2B cofactor is stable over the 50-ns time scale of the simulations even in the absence of the inhibitor. Moreover, the β 2- β 3 loop of NS2B shows limited flexibility (Fig. 2, top). In the inhibitor-bound conformation, the tips of the NS2B β 2- β 3 loop and NS3pro E1B-F1 loop are in contact (blue structure in Fig. 2, top). The separation of the two tips can be monitored by the distance between the C_{α} atoms of NSB2 Asp82 and NS3pro Lys73 (C_{α} - C_{α} distance of 5.0 and 5.4 Å in the complex with the tetrapeptide-aldehyde inhibitor [2fp7] and BPTI [2ijo], respectively). Interestingly, the simulations of free (started from the active conformation) and inhibitor-bound NS2B-NS3pro enzyme show similar distribution of the values of this distance which is slightly broader in the runs without inhibitor (see Fig. 3). The higher distribution for values

below 5 Å originates from a closure at about 7.5 ns of the β 2- β 3 loop of NS2B in the 20-ns run of the free enzyme (which yields the peak at about 4.5 Å in the histogram in Fig. 3, bottom). The similar flexibility of the NS2B β 2- β 3 loop in the simulations with and without inhibitor (Fig. 3 and Supporting Information Fig. S2) indicate that the active conformation of NS2B is structurally stable.

Flexibility of the β 2- β 3 loop of NS2B in the simulations started from the inactive conformation

There is a significantly larger displacement of the β 2- β 3 loop of NS2B in the simulations started from the inactive (Fig. 2, bottom) than the active conformation (Fig. 2, top). The C_{α} RMSD of residues Leu79-Phe85 is almost always higher than 5 Å in the runs started from the inactive conformation (Supporting Information Fig. S2). The opposite, that is, C_{α} RMSD below 5 Å, is observed for the runs from the active conformation. As mentioned earlier, this loop is involved in extensive crystal contacts in the 2ggv structure (inactive) but not in the 2fp7 structure (active).

Fluctuations of the NS2B β 2- β 3 loop and correlated motion of active site loops facilitate substrate binding

Reversible local motion of the β 2- β 3 loop of NS2B on the 10-ns time scale is observed in the MD runs of the

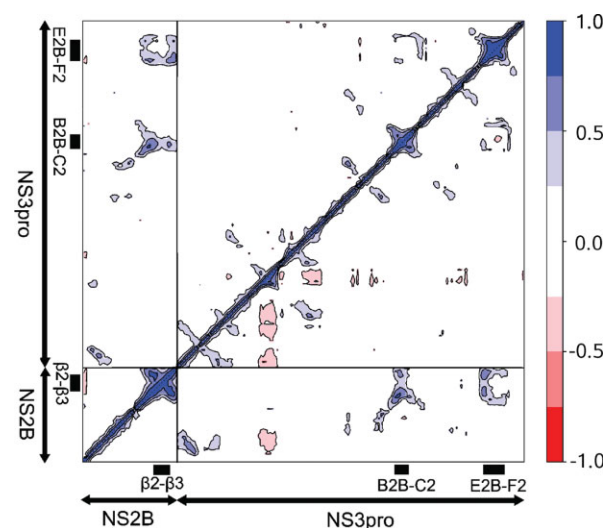


Figure 4. Correlated motion in the NS2B and NS3pro loops adjacent to the active site. To evaluate the statistical noise, that is, sampling robustness, two simulation intervals were analyzed: The 15–30 ns (top, left triangular matrix) and 55–70 ns (bottom, right triangular matrix) intervals of the 80-ns MD run started from the active conformation without inhibitor. They show similar motional correlations, that is, high symmetry with respect to the diagonal, except for some slightly anticorrelated motion present only in the latter interval. The color range varies from blue (fully correlated motion) to red (fully anticorrelated) as indicated on the color bar on the right. [Color figure can be viewed in the online issue, which is available at www.interscience.wiley.com.]

free enzyme (Fig. 3, top and Supporting Information Fig. S2). As an example, an opening and closing event takes place in the first half of the 80-ns run started from the active conformation of NS2B (Fig. 2, top). The 10-ns time scale and amplitude of this motion are of similar magnitude as observed for loops of other enzymes in previous simulation studies^{13–15} [note the similar time scales and amount of displacement in the NS2B loop (Fig. 2, top) and the flap of a human aspartic protease Fig. 5 of Ref. 14] and experimental investigations.¹⁶ As the NS2B β 2- β 3 loop (in its active conformation) is located between the E2B-F2 and B2B-C2 loops of NS3pro it is worth to investigate eventual correlated displacements. Covariance matrix analysis (see “Methods” section) of the MD trajectories started from the active conformation shows correlated motion between the β 2- β 3 loop of NS2B and the two loops of NS3pro (see Fig. 4). The fluctuations of the β 2- β 3 loop and correlated motion with the NS3pro loops are likely to promote substrate binding and release by full formation and partial opening of the S_2 and S_3 pockets. Note that this suggestion goes beyond the available experimental evidence because the two X-ray structures of inhibitor-bound WNV NS2B-NS3pro enzyme show a perfect overlap in the β 2- β 3 loop of NS2B despite the different sizes and steric requirements of BPTI (2ijo)¹⁰ and the tetrapeptide-aldehyde inhibitor (2fp7).⁸ Furthermore, the partial and reversible opening of the NS2B β 2- β 3 loop observed in the MD runs started from the active conformation is a much smaller motion than the NS2B displacement postulated by comparing the X-ray structures of the free (2ggv) and inhibitor-bound (2fp7, 2ijo) WNV NS2B-NS3pro enzyme.

Displacement of the E2B-F2 loop of NS3pro from the orientation in the X-ray structure of the free enzyme

In all simulations started from the inactive conformation there is a displacement of the E2B-F2 loop of NS3pro towards the B2B-C2 loop (Fig. 2, bottom) where the former occludes the cavity that is occupied by the β 2- β 3 loop of NS2B in the inhibitor bound structure. This displacement brings the E2B-F2 loop in the same orientation as in the inactive structure of Dengue NS3pro (PDB code 2fom) as shown by the small value of the C_α RMSD of residues Val154-Ile162 from the inactive structure of Dengue NS3pro (Supporting Information Fig. S3). The orientation of the E2B-F2 loop of WNV NS3pro in the inactive X-ray structure (2ggv) is kept in place by extensive crystal contacts (see Fig. 1) due to a symmetric dimer which is most probably a crystallization artifact.¹⁰

Evidence for conformational selection in the oxyanion hole (S_1)

As mentioned in the Introduction, of the three crystal structures of WNV NS2B-NS3pro only the complex with BPTI (2ijo) has a catalytically competent oxyanion hole

with the backbone NH groups of residues 133–135 pointing into the hole (green structure in Fig. 5, top). On the other hand, both X-ray structures used in the MD simulations (2fp7 and 2ggv) show a nonproductive orientation of the NH group of residue 133. The spontaneous reorientation of the Thr132-Gly133 peptide bond that results in the formation of the catalytically competent oxyanion hole is observed in three (of the four) MD runs started from the enzyme structure with the β 2- β 3 loop of NS2B far away from the active site (see Fig. 5) as well as in two MD runs initiated from the active conformation of NS2B (not shown). The full formation of the oxyanion hole is irreversible in the time scale of the MD simulations. Therefore, the simulations without inhibitor indicate that the catalytically competent oxyanion hole is structurally stable, which is not consistent with the postulated induced-fit mechanism. In other words, this MD result is in net contrast with the suggestion that the nonproductive conformation of the hole is favored in the absence of substrate,¹⁰ which was based on the differences observed in the X-ray structures with the tetrapeptide-aldehyde inhibitor⁸ and BPTI.¹⁰

Evidence for conformational selection in the S_1 pocket

An aspartate residue (Asp129) is located at the base of the S_1 pocket of NS3pro as in most trypsin-like serine proteases. Of the three possible rotamers of the χ_1 angle of Asp129, only the trans (180 degrees) is optimal for salt bridge formation with the P_1 Lys or Arg side chain in the substrate (as in the X-ray structure of the complex with the tetrapeptide-aldehyde inhibitor).⁸ The –60-degree rotamer of Asp129 results in a less favorable orientation for the intermolecular salt bridge than the trans rotamer, whereas the +60-degree rotamer results in an orientation of the side chain with the carboxy group far away from the base of the S_1 pocket. Interestingly, along the MD simulations the χ_1 angle of Asp129 only sporadically assumes the +60 rotamer. It is mainly in the trans and –60 rotamer in the simulations started from the active and inactive conformation, respectively, but frequent transitions are observed between these two states (see Fig. 6). The stability of the Asp129 orientation that favors salt bridge formation with the substrate provides further evidence that WNV NS3pro binds the substrate by a conformational selection mechanism rather than induced fit.

Discussion

A precise balance between structural plasticity and stability is required for the efficient activity of most enzymes. We have performed MD simulations to investigate the flexibility and relative stability of the inhibitor-bound and inhibitor-free X-ray structures of the WNV NS2B-NS3pro enzyme, which differ significantly in the position and orientation of the β 2- β 3 loop of the NS2B cofactor. In the crystal structure of WNV NS2B-NS3pro in the complex with a

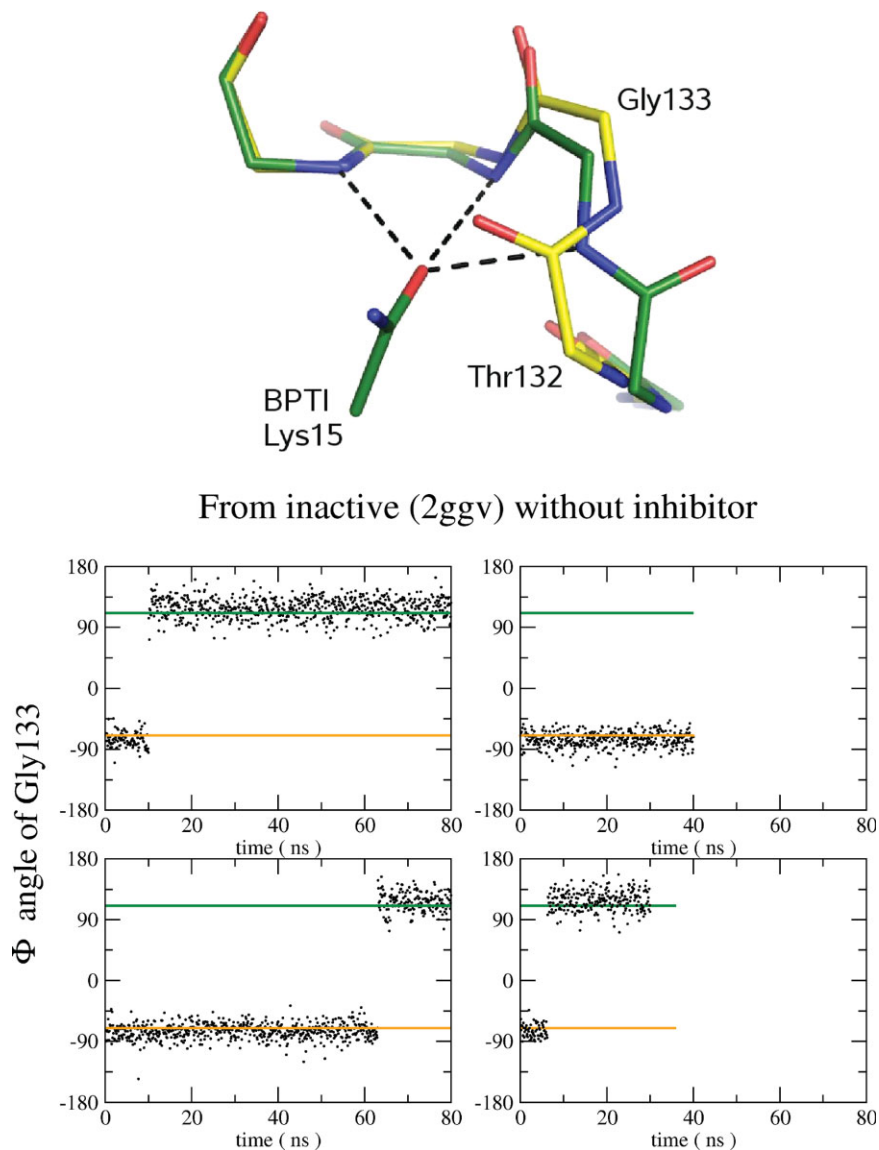


Figure 5. Spontaneous formation of the oxyanion hole during three of the four MD simulations started from the inactive conformation. (Top) The structures with yellow (2fp7) and green (2ijo) carbon atoms are shown to illustrate the nonproductive and productive orientation of the Thr132-Gly133 peptide bond, respectively. (Bottom) The same colors are used for the horizontal lines in the time series of the ϕ angle of Gly133 which reflects the orientation of the NH group whose flip produces the catalytically competent conformation of the oxyanion hole. [Color figure can be viewed in the online issue, which is available at www.interscience.wiley.com.]

tetrapeptide-aldehyde inhibitor (PDB code 2fp7) the β 2- β 3 loop is part of the active site (and this conformation is referred to as active), whereas in the X-ray structure of the free enzyme (2ggv, termed inactive) its tip is located at a distance of about 50 Å and protrudes towards the solvent though it is stabilized in part by crystal contacts. Three main observations emerge from the analysis of the MD trajectories and comparison with the available crystal structures. First, the active conformation of the NS2B β 2- β 3 loop is stable on a 50-ns time scale even in the absence of the inhibitor. Furthermore, it is less flexible in MD runs started from the active structure than the inactive. These simulation results provide strong evidence that the conformation of the NS2B-NS3pro enzyme with

the NS2B β 2- β 3 loop as part of the active site is a (meta)stable state. Furthermore, these observations justify the use of the active structure for high-throughput docking, which has resulted in the recent discovery of nonpeptidic inhibitors.¹⁷

Second, the MD simulations started from the active conformation indicate that the partial and reversible opening of the NS2B β 2- β 3 loop and its correlated motion with the adjacent NS3pro E2B-F2 loop are involved in substrate binding and product release. As these loops make up the S₂-S₄ pockets of the NS2B-NS3pro complex the reversible motion is likely to facilitate the binding of the nonprime part of the polypeptide substrate to the active conformation of the NS2B-NS3pro enzyme.

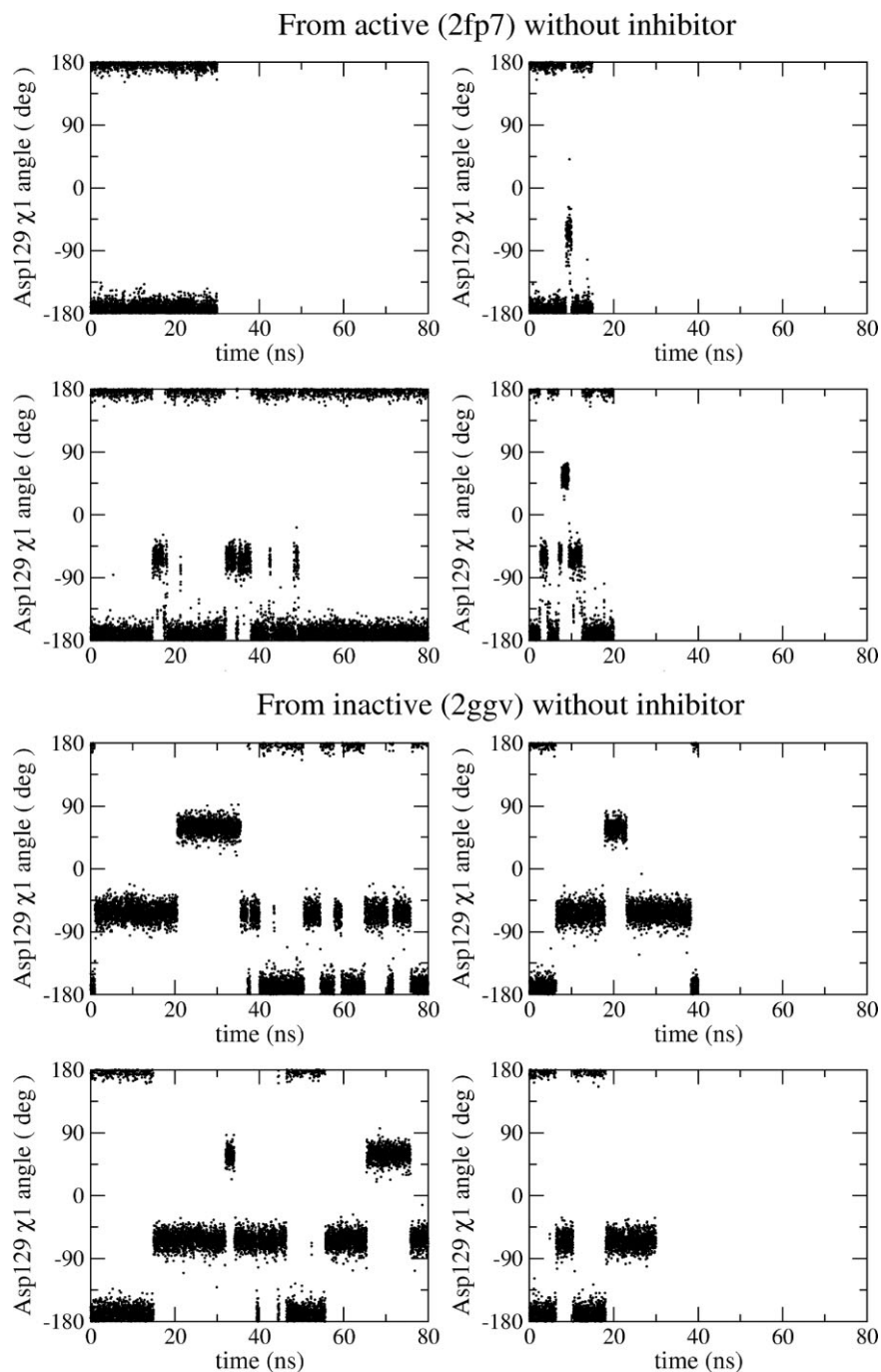


Figure 6. The orientation of the S_1 side chain Asp129 favors intermolecular salt bridge formation. Note that only the +60-degree rotamer, which is sporadic, does not allow the salt bridge between Asp129 and the Arg or Lys side chain at position P_1 of the substrate or peptidic inhibitor.

Third, the catalytically competent conformation of the S_1' and S_1 pockets is more stable than the nonproductive counterpart. In fact, the spontaneous and irreversible formation of the catalytically competent oxyanion hole at the S_1' pocket is observed in five of eight MD simulations. Furthermore, the Asp129 side chain at the bottom of the S_1 pocket switches rapidly in-and-out of an orientation that favors binding of a positively charged side chain (P_1 of substrate), and is observed most of the time in the productive orientation. Therefore, the MD simulations indicate that the natural sub-

strate and the known peptide inhibitors of the two-component flaviviral enzyme NS2B-NS3pro bind to a (meta)stable conformation rather than by inducing a large conformational transition.

Material and Methods

MD simulations

The coordinates of the inhibitor-free WNV NS3pro-NS2B protease¹⁰ and its complex with the tetrapeptide inhibitor Bz-Nle-Lys-Arg-Arg-H⁸ were downloaded

from the PDB database (entries [2ggv](#) and [2fp7](#), respectively). Only the complex with the tetrapeptide inhibitor was available (but not the BPTI complex) when this study was initiated, which explains why the [2fp7](#) (and not [2ijo](#)) structure was used for the simulations from the active conformation. All termini, including those next to the segment missing in the [2fp7](#) X-ray structure (residues 28–32 of NS3pro), were neutralized by the $-\text{COCH}_3$ group and the $-\text{NHCH}_3$ group at the N-terminus and C-terminus, respectively. To reproduce neutral pH conditions the side chains of aspartates and glutamates were negatively charged, those of lysines and arginines were positively charged, and histidines were considered neutral. The protein was immersed in an orthorhombic box of preequilibrated water molecules. The size of the box was chosen to have a minimal distance of 13 Å between the boundary and any atom of the protein. The simulation system contained 10 (or seven in the peptidic inhibitor complex system) sodium cations to compensate for the net negative charge of the NS3pro/NS2B complex. The program VMD¹⁸ was used for setting up the simulation system, while minimization, heating and production runs were performed with NAMD²¹⁹ using the CHARMM22 force field²⁰ and the TIP3P model of water. Periodic boundary conditions were applied and the particle-mesh Ewald approach²¹ was used for the long-range electrostatics. The van der Waals interactions were truncated at a cutoff of 12 Å and a switch function was applied starting at 10 Å. The MD simulations were performed at constant temperature (298 K) and constant pressure (1 atm) with a time step of 2 fs using the SHAKE algorithm²² to fix the length of covalent bonds involving hydrogen atoms.

Analysis of MD simulations

The analysis of the trajectories was performed with CHARMM,²³ and the program WORDOM²⁴ which is particularly efficient in handling large sets of trajectories. Dynamical cross-correlation matrices were calculated using the Bio3d package²⁵ within the R environment for statistical computing.²⁶

Acknowledgments

The authors thank Dr. Danzhi Huang for useful discussions and comments to the manuscript. They are grateful to Armin Widmer (Novartis Basel) for the continuous support with the program WITNOTP which was used for visual analysis of the trajectories. The MD simulations were performed on the Matterhorn Beowulf cluster at the Informatikdienste of the University of Zurich.

References

- Centers for Disease Control and Prevention (2007) Division of vector-borne infectious disease. West Nile virus homepage. Centers for Disease Control and Prevention. Available at: <http://www.cdc.gov/ncidod/dvbid/westnile>.

- Mukhopadhyay S, Kuhn RJ, Rossmann MG (2005) A structural perspective of the flavivirus life cycle. *Nat Rev Microbiol* 3:13–22.
- Chappell KJ, Stoermer MJ, Fairlie DP, Young PR (2006) Insights to substrate binding and processing by West Nile Virus NS3 protease through combined modeling, protease mutagenesis, and kinetic studies. *J Biol Chem* 281:38448–38458.
- Perni RB, Almquist SJ, Byrn RA, Chandorkar G, Chaturvedi PR, Courtney LF, Decker CJ, Dinehart K, Gates CA, Harbeson SL, Heiser A, Kalkeri G, Kolaczowski E, Lin K, Luong Y-P, Rao BG, Taylor WP, Thomson JA, Tung RD, Wei Y, Kwong AD, Lin C (2006) Preclinical profile of VX-950, a potent, selective, and orally bioavailable inhibitor of hepatitis C virus NS3-4A serine protease. *Antimicrob Agents Chemother* 50:899–909.
- Tomei L, Failla C, Santolini E, Francesco RD, Monica NL (1993) NS3 is a serine protease required for processing of hepatitis C virus polyprotein. *J Virol* 67:4017–4026.
- Malcolm BA, Liu R, Lahser F, Agrawal S, Belanger B, Butkiewicz N, Chase R, Gheyas F, Hart A, Hesk D, Ingravallo P, Jiang C, Kong R, Lu J, Pichardo J, Prongay A, Skelton A, Tong X, Venkatraman S, Xia E, Girijavallabhan V, Njoroge FG (2006) SCH 503034, a mechanism-based inhibitor of hepatitis C virus NS3 protease, suppresses polyprotein maturation and enhances the antiviral activity of alpha interferon in replicon cells. *Antimicrob Agents Chemother* 50:1013–1020.
- Seiwert S, Andrews S, Jiang Y, Serebryany V, Tan H, Kossen K, Rajagopalan P, Misialek S, Stevens S, Stoycheva A, Hong J, Lim S, Qin X, Rieger R, Condroski K, Zhang H, Do M, Lemieux C, Hingorani G, Hartley D, Josey J, Pan L, Beigelman L, Blatt L (2008) Preclinical characteristics of the HCV NS3/4A protease inhibitor ITMN-191 (R7227) in press. *Antimicrob Agents Chemother* 52:4432–4441.
- Erbel P, Schiering N, Hommel U (2006) Structural basis for the activation of flaviviral NS3 proteases from dengue and West Nile virus. *Nat Struct Mol Biol* 13:372–373.
- Yusof R, Clum S, Wetzel M, Murthy HM, Padmanabhan R (2000) Purified NS2B/NS3 serine protease of dengue virus type 2 exhibits cofactor NS2B dependence for cleavage of substrates with dibasic amino acids in vitro. *J Biol Chem* 275:9963–9969.
- Aleshin AA, Shiryaev SA, Strongin AY, Liddington RC (2007) Structural evidence for regulation and specificity of flaviviral proteases and evolution of the Flaviviridae fold. *Protein Sci* 16:1–12.
- Niyomrattanakit P, Winoyanuwattikun P, Chanprapaph S, Angsuthanasombat C, Panyim S, Katzenmeier G (2004) Identification of residues in the dengue virus type 2 NS2B cofactor that are critical for NS3 protease activation. *J Virol* 78:13708–13716.
- Zuo Z, Liew OW, Chen G, Chong PCJ, Lee SH, Chen K, Jiang H, Puah CM, Zhu W (2009) Mechanism of NS2B-mediated activation of NS3pro in dengue virus: molecular dynamics simulations and bioassays. *J Virol* 83:1060–1070.
- Levy Y, Caflish A (2003) Flexibility of monomeric and dimeric HIV-1 protease. *J Phys Chem B* 107:3068–3079.
- Gorfe AA, Caflish A (2005) Functional plasticity in the substrate binding site of β -secretase (BACE). *Structure* 13:1487–1498.
- Friedman R, Caflish A (2008) Pepsinogen-like activation intermediate of plasmepsin II revealed by molecular dynamics analysis. *Proteins: Struct Funct Bioinformatics* 73:814–827.

16. Henzler-Wildman KA, Lei M, Thai V, Kerns J, Karplus M, Kern D (2008) A hierarchy of timescales in protein dynamics is linked to enzyme catalysis. *Nature* 450: 913–916.
17. Ekonomiuk D, Su X-C, Ozawa K, Bodenreider C, Lim SP, Yin Z, Keller TH, Beer D, Patel V, Otting G, Caflisch A, Huang D (2009) Discovery of a non-peptidic inhibitor of West Nile virus NS3 protease by high-throughput docking. *PLoS Negl Trop Dis* 3:e356.
18. Humphrey W, Dalke A, Schulten K (1996) Vmd: visual molecular dynamics. *J Mol Graph* 33:27–28.
19. Phillips JC, Braun R, Wang W, Gumbart J, Tajkhorshid E, Villa E, Chipot C, Skeel RD, Kalé L, Schulten K (2005) Scalable molecular dynamics with NAMD. *J Comput Chem* 26:1781–1802.
20. MacKerell Jr A, Bashford D, Bellott M, Dunbrack R Jr, Field M, Fischer S, Gao J, Guo H, Ha S, Joseph D, Kuchnir L, Kuczera K, Lau F, Mattos C, Michnick S, Ngo T, Nguyen D, Prodhom B, Roux B, Schlenkrich M, Smith J, Stote R, Straub J, Wiorcikiewicz-Kuczera J, Karplus M (1998) All-atom empirical potential for molecular modeling and dynamics studies of proteins. *J Phys Chem B* 102:3586–3616.
21. Essmann U, Perera L, Berkowitz ML, Darden T, Lee H, Pedersen LG (1995) A smooth particle mesh Ewald method. *J Chem Phys* 103:8577–8593.
22. Ryckaert JP, Ciccotti G, Berendsen HJC (1977) Numerical integration of the Cartesian equation of motion of a system with constraints: molecular dynamics of *n*-alkanes. *J Comp Phys* 23:327–341.
23. Brooks BR, Bruccoleri RE, Olafson BD, States DJ, Swaminathan S, Karplus M (1983) CHARMM: a program for macromolecular energy, minimization, and dynamics calculations. *J Comput Chem* 4:187–217.
24. Seeber M, Cecchini M, Rao F, Settanni G, Caflisch A (2007) Wordom: a program for efficient analysis of molecular dynamics simulations. *Bioinformatics* 23: 2625–2627.
25. Grant BJ, Rodrigues APC, ElSawy KM, McCammon JA, Caves LSD (2006) Bio3d: an R package for the comparative analysis of protein structures. *Bioinformatics* 22: 2695–2696.
26. R Development Core Team (2008) R: a language and environment for statistical computing. Vienna, Austria: R Foundation for Statistical Computing. ISBN 3-900051-07-0.